Polymer 51 (2010) 4806–4813

Contents lists available at ScienceDirect

Polymer

journal homepage: www.elsevier.com/locate/polymer

Star-like poly(*n*-butyl acrylate)-*b*-poly(α-methylene-γ-butyrolactone) block copolymers for high temperature thermoplastic elastomers applications

Azhar Juhari [a], Jaroslav Mosnáček [b,c], Jeong Ae Yoon [b], Alper Nese [b], Kaloian Koynov [a], Tomasz Kowalewski [b], Krzysztof Matyjaszewski [b,*]

[a] Max Planck Institute for Polymer Research, Ackermannweg 10, 55128 Mainz, Germany
[b] Department of Chemistry, Carnegie Mellon University, 4400 Fifth Avenue, Pittsburgh, PA, 15213, USA
[c] Polymer Institute, Slovak Academy of Sciences, Dúbravská cesta 9, 842 36 Bratislava, Slovakia

ARTICLE INFO

Article history:
Received 2 July 2010
Received in revised form
5 August 2010
Accepted 8 August 2010
Available online 14 August 2010

Keywords:
ATRP
Block copolymers
Thermoplastic elastomers

ABSTRACT

Thermoplastic elastomers based on well-defined 10- and 20 arm star-like block copolymers containing middle soft poly(*n*-butyl acrylate) (PBA) block and outer hard poly(α-methylene-γ-butyrolactone) (PMBL) block were synthesized by atom transfer radical polymerization (ATRP). Phase separated cylindrical or lamellar morphologies, depending on the copolymers composition and the annealing temperature of the films, were observed by atomic force microcopy and small-angle X-ray scattering. The mechanical and thermal properties of the copolymers were thoroughly characterized. The prepared copolymers retained their phase separated morphology even at temperatures exceeding 300 °C. Both tensile strength and elongation values for the star-like copolymers were considerably higher than for linear copolymers with similar composition.

1. Introduction

Thermoplastic elastomers (TPEs) are materials combining elastomeric behavior under the service conditions with thermoplastic properties above the order–disorder transition (ODT) temperatures [1–3]. The most common conventional TPEs are polystyrene-*b*-polybutadiene-*b*-polystyrene (SBS) or polystyrene-*b*-polyisoprene-*b*-polystyrene (SIS) block copolymers. However, these TPEs have some drawbacks such as poor chemical, heat, and UV resistance due to the unsaturated soft blocks as well as low service temperature limited by glass transition temperature (T_g) of the polystyrene block (ca. 100 °C) [4]. Therefore there have been continuous efforts to overcome these drawbacks by substitution of polybutadiene or polyisoprene with more stable soft blocks and polystyrene with polymers having higher T_g. In order to increase service temperature, various hard blocks such as poly (4-tert-butylstyrene) [5], poly (α-methylstyrene) [6], poly(4-(1-adamantyl)styrene) [7] or polyindene [8] were employed to substitute polystyrene blocks of SBS or SIS copolymers. In addition, various fully acrylic TPEs based on combination of polyacrylates as soft blocks with polymethacrylates as hard blocks were prepared by controlled polymerization techniques [9–15]. These polymers are not sensitive to UV and oxidation. Moreover the combination of various (meth) acrylic monomers offer materials with a wide range of T_g from ca. - 50 to + 200 °C.

Recently, atom transfer radical polymerization (ATRP) [16–20] was used for the preparation of well-defined block copolymers of α-methylene-γ-butyrolactone (MBL) [15,21]. MBL, found in tulips, is the simplest member of butyrolactones isolated from various plants [22–24]. PMBL possesses interesting properties such as good durability, a high refractive index (1.540) and high T_g (195 °C) [25,26]. Various copolymers and blends containing MBL units have good optical properties and resistances to heat, weathering, scratches, and solvents [27]. These properties can be beneficial for the use of PMBL as a hard component in thermoplastic properties. Preparation and study of properties of linear triblock PMBL copolymers with soft poly (*n*-butyl acrylate) (PBA) control segments were recently published [15]. These copolymers showed elastic properties up to 200 °C, however their mechanical properties were relatively poor due to brittleness of PMBL block [27,28].

Thermoplastic elastomers based on star block copolymers may possess improved properties in comparison with their linear counterparts (linear ABA triblock copolymers), in respect to mechanical properties, sensitivity to diblock contamination as well as lower melt viscosities and thus better processibility [8,29–34]. Herein we report preparation of star-like block copolymers consisting of inner soft PBA blocks and outer hard PMBL blocks. We have studied the morphology

* Corresponding author. Tel.: +1 412 268 3209; fax: +1 412 268 6897.
E-mail address: km3b@andrew.cmu.edu (K. Matyjaszewski).

0032-3861/$ – see front matter © 2010 Elsevier Ltd. All rights reserved.
doi:10.1016/j.polymer.2010.08.017

and the thermal and mechanical properties of the prepared copolymers and compared their thermoplastic elastomer characteristics with those of the corresponding linear triblock ABA copolymers.

2. Experimental

2.1. Materials

All monomers were purified by passing through a basic alumina column to remove the inhibitor. CuCl was purified according to the literature procedures [35]. $CuCl_2$ and ligand 2,2′-bipyridine (bpy) [16] (all from Aldrich) were used as received. All other reagents and solvents were purchased from Aldrich and used as received without further purification. Poly (2-bromoisobutyryloxyethyl acrylate-*graft*-butyl acrylate)s (PBiBEA-*g*-PBA) star-like macroinitiators were synthesized as described previously (see Scheme 1) [34].

2.2. Synthesis of poly (2-bromoisobutyryloxyethyl acrylate-graft-(butyl acrylate-block-α-methylene-γ-butyrolactone))s, PBiBEA-g-(PBA-b-PMBL)

The general procedure for the chain extension of the PBiBEA-*g*-PBA macroinitiator was as follows: a round bottom flask containing MBL, PBiBEA-*g*-PBA macroinitiator, $CuCl_2$, bpy, and DMF was degassed by three freeze-pump-thaw cycles. Then, CuCl was added to the frozen reaction solution under nitrogen flow. The flask was closed, evacuated, back-filled with nitrogen, and immersed in an oil bath thermostated at 50 °C. Molar ratios of monomer: initiator: CuCl: $CuCl_2$: ligand are described in Table 1 (Entries C1–C10). After the polymerization was stopped, DMF was added and the polymer solution was purified by passing through a neutral alumina column. The final polymer was precipitated twice from DMF into methanol.

2.3. General analysis

Monomer conversions and molecular weights of the copolymers were determined by ^{1}H NMR on a 300 MHz Bruker NMR spectrometer using deuterated DMF as a solvent. The molecular weight distributions of the polymers were measured using a GPC (Polymer Standards Services (PSS) columns (guard, 10^5, 10^3, and 10^2 Å) with DMF (containing 5 mM LiBr) as an eluent at 50 °C, flow rate 1.00 mL/min, and differential refractive index (RI) detector (Waters, 2410)). Polystyrene (PS) was used as a calibration standard employing WinGPC software from Polymer Standards Service. Toluene was used as the internal standard to correct for any fluctuation in DMF flow rate.

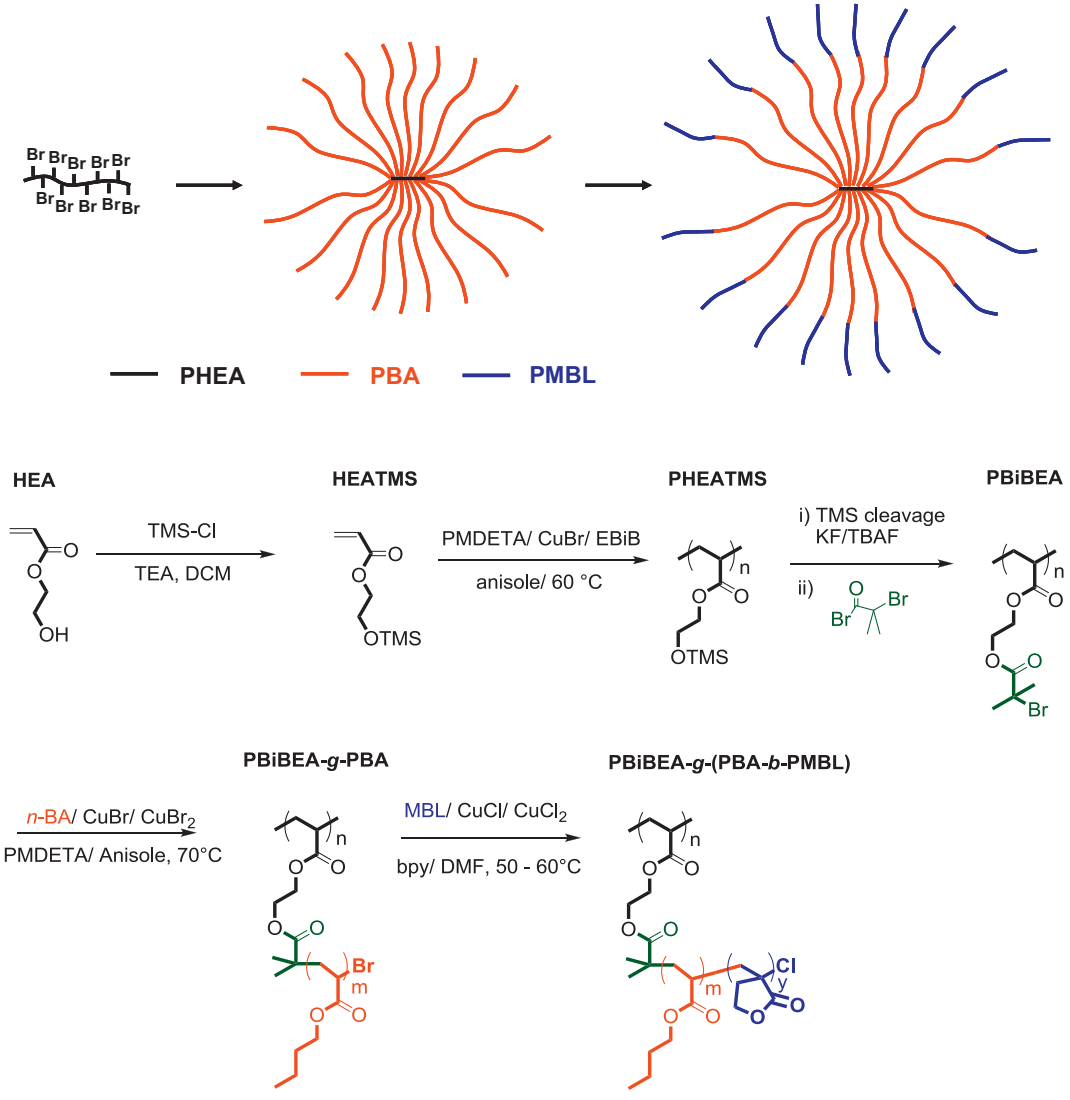

Scheme 1. Synthesis of graft copolymers.

Table 1
Experimental conditions of ATRP of MBL during arms extension of PBiBEA-*g*-PBA star-like polymers, and characterization of prepared polymers.

Entry	AL	I	CuCl	$CuCl_2$	L	DMF vol%	T (°C)	Time (h)	Conv.[f] (%)	$M_{n,\ exp.}$[f]	M_w/M_n[g]
1	110	1 (10B115)[a]	1.5	0.2	3.4	62	50	7.5	25	179 000	1.20
2	110	1 (10B115)[a]	1.5	0.2	3.4	62	50	10.5	44	196 000	1.24
3	240	1 (10B240)[b]	1.5	0.2	3.4	62	50	15	21	355 000	1.21
4	240	1 (10B240)[b]	1.5	0.2	3.4	62	50	28	40	394 000	1.25
5	110	1 (20B115)[c]	1.8	0.15	3.9	62	50	5	40	391 000	1.37
6	110	1 (20B115)[c]	1.8	0.15	3.9	62	50	6.5	53	411 000	1.46
7	150	1 (10B230)[d]	1.8	0.15	3.9	57	60	29	55	782 000	1.49
8	980	1 (20B750)[e]	2.0	0.2	4.4	62	60	140	21	2 230 000	NA

AL, I and L stand for α-methylene-γ-butyrolactone (MBL), PBiBEA-*g*-PBA macroinitiator and bpy, respectively.
[a] $PBiBEA_{10}$-*g*-PBA_{115} macroinitiator with $M_n = 147\ 000$ g/mol, $M_w/M_n = 1.15$.
[b] $PBiBEA_{10}$-*g*-PBA_{240} macroinitiator with $M_n = 308\ 000$ g/mol, $M_w/M_n = 1.15$.
[c] $PBiBEA_{20}$-*g*-PBA_{115} macroinitiator with $M_n = 294\ 000$ g/mol, $M_w/M_n = 1.14$.
[d] $PBiBEA_{20}$-*g*-PBA_{230} macroinitiator with $M_n = 590\ 000$ g/mol, $M_w/M_n = 1.13$.
[e] $PBiBEA_{20}$-*g*-PBA_{750} macroinitiator with $M_n = 1\ 920\ 000$ g/mol, $M_w/M_n = 1.21$.
[f] Based on ^1H NMR spectra.
[g] Based on GPC using PS standards.

2.4. Tapping Mode Atomic Force Microscopy (TMAFM)

For a phase separated film morphology investigation, the block copolymers were dissolved in DMF (1 mg/mL) and were deposited by drop casting onto silicon wafer surface (1 cm × 1 cm) cleaned by rinsing with acetone and isopropanol followed by oxygen plasma treatment. The samples were dried in a vacuum oven at room temperature overnight. Tapping mode AFM experiments were carried out using a Dimension V scanning probe microscope with a NanoScope V controller (Veeco). The measurements were performed in air using commercial Si cantilevers with a nominal spring constant and resonance frequency of 42 N/m and 330 kHz, respectively. The height and phase images were acquired simultaneously at a set-point ratio $A/A_0 = 0.7–0.8$, where A and A_0 refer, respectively, to the "tapping" and "free" cantilever amplitude. For investigations of morphology changes by annealing, samples used for AFM observations were annealed at 230 °C for 30 min under nitrogen flow in an oven. After annealing, the oven was turned off and cooled down naturally while maintaining nitrogen flow. The annealed samples were observed by TMAFM under the similar conditions described earlier and figured out the morphology changes.

2.5. Power spectral analysis of TMAFM images

Phase mode AFM images showing contrast periodicities were analyzed by a 2-D Fourier transform (FT). Subsequently, the 2-D FT maps were azimuthally averaged to produce magnitude plots analogous to the scattering patterns. After recalculating the spatial frequency scale to scattering vector units (q, 2π/d), the domain spacing (d) was calculated from the q value that showed the peak maximum of the power spectrum.

2.6. Small-Angle X-ray Scattering analysis (SAXS)

SAXS measurements were conducted using a rotating anode (Rigaku RA-Micro 7) X-ray beam with a pinhole collimation and a two-dimensional detector (Bruker Highstar) with 1024 × 1024 pixels. A double graphite monochromator for the Cu Kα radiation ($\lambda = 0.154$ nm) was used. The beam diameter was about 0.8 mm, and the sample to detector distance was 1.8 m. The recorded scattered intensity distributions were integrated over the azimuthal angle and are presented as functions of the scattering vector ($s = 2\sin(\theta)/\lambda$, where 2θ is the scattering angle).

2.7. Dynamic Mechanical Analysis (DMA)

DMA was performed on a Rheometrics RMS 800 mechanical spectrometer. Shear deformation was applied under conditions of controlled deformation amplitude, which was kept in the range of the linear viscoelastic response of studied samples. Plate–plate geometry was used with plate diameters of 6 mm. Experiments have been performed under a dry nitrogen atmosphere. Results are presented as temperature dependencies of the storage (G') and loss (G'') shear moduli measured at a constant deformation frequency of 10 rad/s. The results were obtained with a 2 °C/min heating rate.

2.8. Tensile tests

Tensile tests were performed using a mechanical testing machine Instron 6000. Samples with thickness in the order of 0.2–0.5 mm were drawn with the rate of 5 mm/min at room temperature. Dependencies of stress vs. draw ratio were recorded. Elastic modulus, elongation at break and stress at break were determined by averaging of 3–5 independent drawing experiments performed at the same conditions.

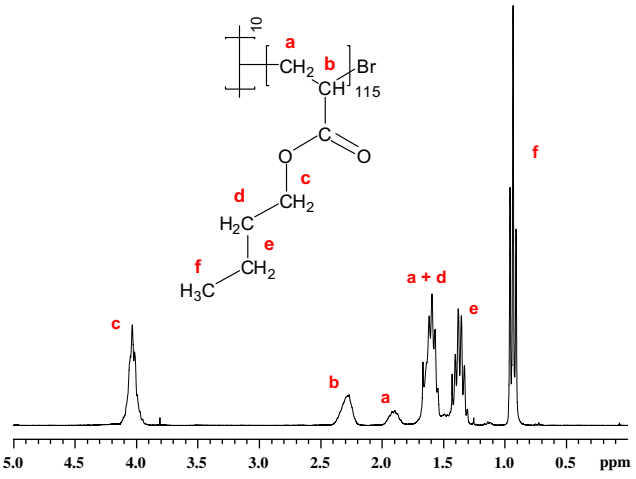

Fig. 1. ^1H NMR spectra of $PBiBEA_{10}$-*g*-PBA_{115} in $CDCl_3$.

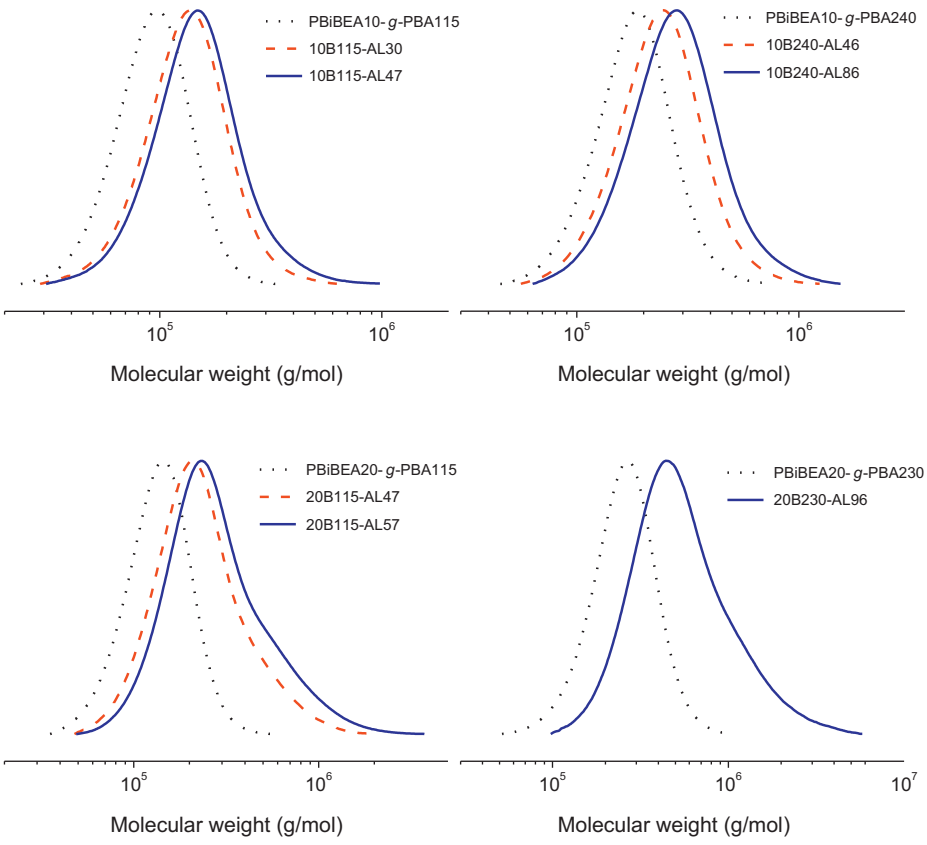

Fig. 2. GPC traces of PBiBEA-*g*-(PBA-*b*-PMBL) star-like block copolymers prepared by arms extension from PBiBEA-*g*-PBA star-like macroinitiators.

3. Results and discussion

3.1. Synthesis

PBiBEA-*g*-PBA star-like macroinitiators were prepared in four steps like described in our previous paper (see Scheme 1) [34]. Briefly, as a first step of the synthesis, an alcohol group of 2-hydroxyethyl acrylate (HEA) was protected with trimethylsilyl group (TMS) giving the monomer trimethylsilyloxyethyl acrylate (HEATMS). HEATMS was polymerized by ATRP technique using ethyl 2-bromoisobutyrate (EBiB) initiator, *N,N,N′,N″,N″*-pentamethyldiethylenetriamine (PMDETA)/CuBr catalyst system and anisole as a solvent. Degree of polymerization of the oligomers determined from ^{1}H NMR spectra was equal to 10 and 20. In the

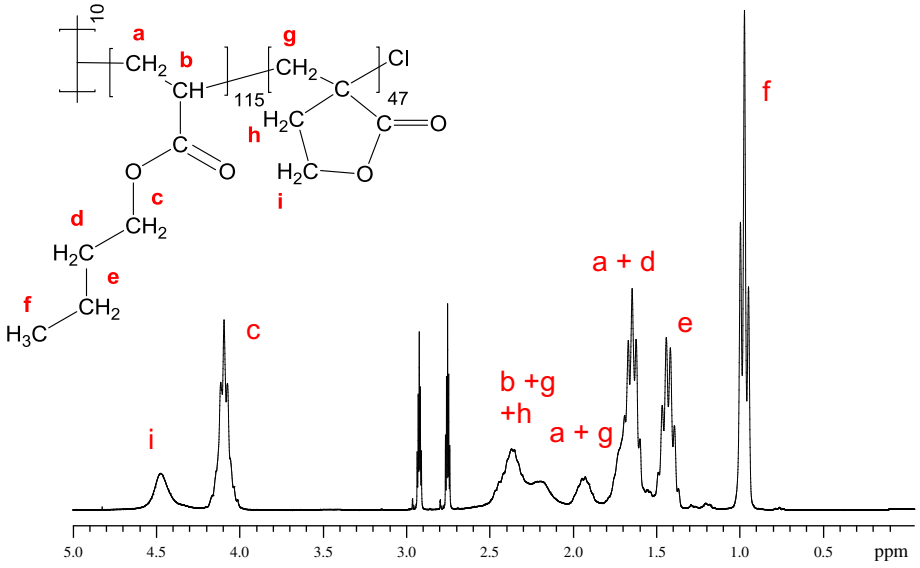

Fig. 3. ^{1}H NMR spectra of 10B115-AL47 (PBiBEA$_{10}$-*g*-(PBA$_{115}$-*b*-PMBL$_{47}$)) in DMF-d$_7$.

Table 2
Composition of the prepared PBiBEA-*g*-(PBA-*b*-PMBL) star-like block copolymers and their phase separation spacing values in thin films.

Entry	Label	Triblock composition	PMBL (mol %)[a]	PMBL (wt %) [a]	Spacing (nm)			Type of morphology form SAXS
					AFM[b]		SAXS	
1	10B115-AL30	$PBiBEA_{10}$-$(PBA_{115}$–$PMBL_{30})_{10}$	20.7	16.5	34	34	25.3	cylinders
2	10B115-AL47	$PBiBEA_{10}$-$(PBA_{115}$–$PMBL_{47})_{10}$	29.0	24.2	41	44	28.5	cylinders
3	10B240-AL46	$PBiBEA_{10}$-$(PBA_{240}$–$PMBL_{46})_{10}$	16.1	12.7	45	51	36.7	cylinders
4	10B240-AL86	$PBiBEA_{10}$-$(PBA_{240}$–$PMBL_{86})_{10}$	26.4	21.6	53	55	42.1	lamellar
5	20B115-AL47	$PBiBEA_{20}$-$(PBA_{115}$–$PMBL_{47})_{20}$	29.0	24.2	41	43	28.5	cylinders
6	20B115-AL57	$PBiBEA_{20}$-$(PBA_{115}$–$PMBL_{57})_{20}$	33.1	27.6	44	52	35.3	lamellar
7	20B230-AL96	$PBiBEA_{20}$-$(PBA_{230}$–$PMBL_{96})_{20}$	29.4	24.2	53	60	49.6	no sec. peaks
8	20B750-AL156	$PBiBEA_{20}$-$(PBA_{750}$–$PMBL_{156})_{20}$	17.2	13.7	103	79	73.3	no sec. peaks

[a] Based on ^{1}H NMR spectra.
[b] Analyzed by a 2-D Fourier transform of phase mode images taken before annealing (left) and after annealing (right).

next step, PHEATMS oligomers were esterified with 2-bromoisobutyryl bromide in the presence of KF to give the multibrominated ATRP macroinitiator PBiBEA. For PBA arms growth from the PBiBEA macroinitiators, PMDETA/CuBr catalyst system was used with anisole as a solvent. Reaction temperature was 70 °C for all the PBA polymerizations. Three various monomer: initiator ratios, 300, 700 and 2100, were used for the preparation of stars with various arms length. Polymerizations were stopped at low monomer conversion, between 30 and 40%, in order to minimize the cross-linking of the stars and loss of the end groups of the growing PBA chains. Molecular weight and molecular weight distribution of the PBiBEA-*g*-PBA star-like macroinitiators are reported as footnotes in Table 1. A typical ^{1}H NMR spectrum of the macroinitiator is shown in Fig. 1.

To prepare star-like thermoplastic elastomers, the ATRP technique was used for chain extension of the PBiBEA-*g*-PBA macroinitiators with PMBL blocks. As the ATRP equilibrium constants for tertiary alkyl halides derived from MBL are much higher than those for *n*-BA [36], extension of arms of PBiBEA-*g*-PBA involved the halogen exchange strategy to provide for higher, or at least equal, rate of cross-propagation, in comparison with rate of propagation [18,37]. Experimental conditions for preparation of all studied copolymers are given in Table 1. An evolution of GPC traces with conversion for extension from PBiBEA-*g*-PBA polymers with MBL segments is shown in Fig. 2. A smooth shift of the molecular weight was observed for all samples. Unlike the copolymers having 10 arms, a shoulder formation towards the higher molecular weight region was observed for the copolymers having 20 arms, and assigned to intermolecular radical coupling reactions between the growing arms of the stars. The fraction of coupled stars increased with an arm length (increased with a monomer conversion). During extension of PBiBEA-*g*-PBA stars with the DP of PBA arms equal to 750 (Table 1, Entry 8), intermolecular coupling reactions between PBiBEA-*g*-(PBA-*b*-PMBL) stars formed so big macromolecules that cannot be filtered and injected to GPC column. Majority of the polymer sample was captured in 0.2 μl filter, used before GPC analysis. Degree of polymerization of the PMBL blocks was calculated from ^{1}H NMR spectra based on the ratio of signals from PBA to signals from PMBL (Fig. 3, signal c to signal i). The compositions of the prepared star-like block copolymers determined by NMR are given in Table 2. Entries 1–8 in Table 2 correspond to entries 1–8 in Table 1.

3.2. Morphology of the PBiBEA-g-(PBA-b-PMBL) star-like block copolymers

AFM imaging was performed for all star-like block copolymer films, in order to directly visualize their morphology. Average film thicknesses were around 400 nm, based on the substrate surface area and the deposited polymer weights. All the samples displayed strong phase separation (Fig. 4 a), implying the immiscibility of PBA and PMBL. The block copolymers with relatively low PMBL contents 10B115-AL30 (16.5 wt %), 10B240-AL46 (12.7 wt %) and 20B750-AL156 (13.7 wt %) clearly showed PMBL cylinders dispersed in the continuous PBA phase and oriented either parallel or perpendicular to the substrate. For the samples with higher PMBL contents (21–28 wt %), mixed morphologies of cylinders and lamellae were observed. In particular, the areas of no periodicity in 10B240-AL86 and 20B115-AL57 were assigned to lamellar layers parallel to the substrates. This assignment was further confirmed by the results of the SAXS experiments performed on thick films as discussed below. The power spectral analysis of the AFM images was performed in order to evaluate the domain spacing (*d*). The results summarized in Table 2 clearly show the effect of the copolymer composition. The increase of PMBL block length leads to the increase in the *d*-spacing for the same length of the PBA segment. In all cases, the spacing values were larger than that determined by SAXS, presumably due to the more stretched polymers in the very thin films used for the AFM studies. Interestingly, after annealing of these thin films for 30 min at 230 °C, the phase separated morphologies transformed to cylinders perpendicular to the substrate (Fig. 4 b) for all studied copolymers. Furthermore the values for the domain spacing increased compared to that measured before the annealing.

SAXS analysis of thick films (~0.3 mm) of the PBA-*b*-PMBL star-like copolymers were performed in order to get a better insight on the effect of phase separation and the resulting morphologies. The scattering measurements were first made without thermal treatment of the copolymer films and then repeated after annealing them for 60 min at 150 °C. While in all cases the annealed films exhibited better ordering than the untreated ones, displaying clearer secondary peaks, the type of morphology (e.g. cylindrical or lamellae) did not change due to this thermal treatment.

Typical SAXS spectra are shown in Fig. 5. From the relative positions of the scattering peaks the type of the phase separated morphology was evaluated and is summarized in Table 2. In good agreement with the AFM results, most of the block copolymers revealed morphologies consistent with hexagonally packed cylinders (two scattering peaks at relative positions$s, \sqrt{3}s$) as shown in Fig. 5 for 10B240-AL46 and 20115-AL47. Only the higher PMBL content copolymers 10B240-AL86 and 20B115-AL57 showed clear lamellar structure with scattering peaks occurring at relative positions *s, 2s*. However after further annealing the thick films of these copolymers at 230 °C, i.e. above the glass transition temperature of the PMBL, their SAXS spectra changed and showed scattering peak consistent with hexagonal morphology. This result is in a good agreement with the change of morphology observed by AFM for very thin films of the same copolymers.

3.3. Thermo-mechanical properties of the PBiBEA-g-(PBA-b-PMBL) star-like block copolymers

Characterization of dynamic mechanical properties of the multi-arm stars PBA–PMBL block copolymers was done by measuring the

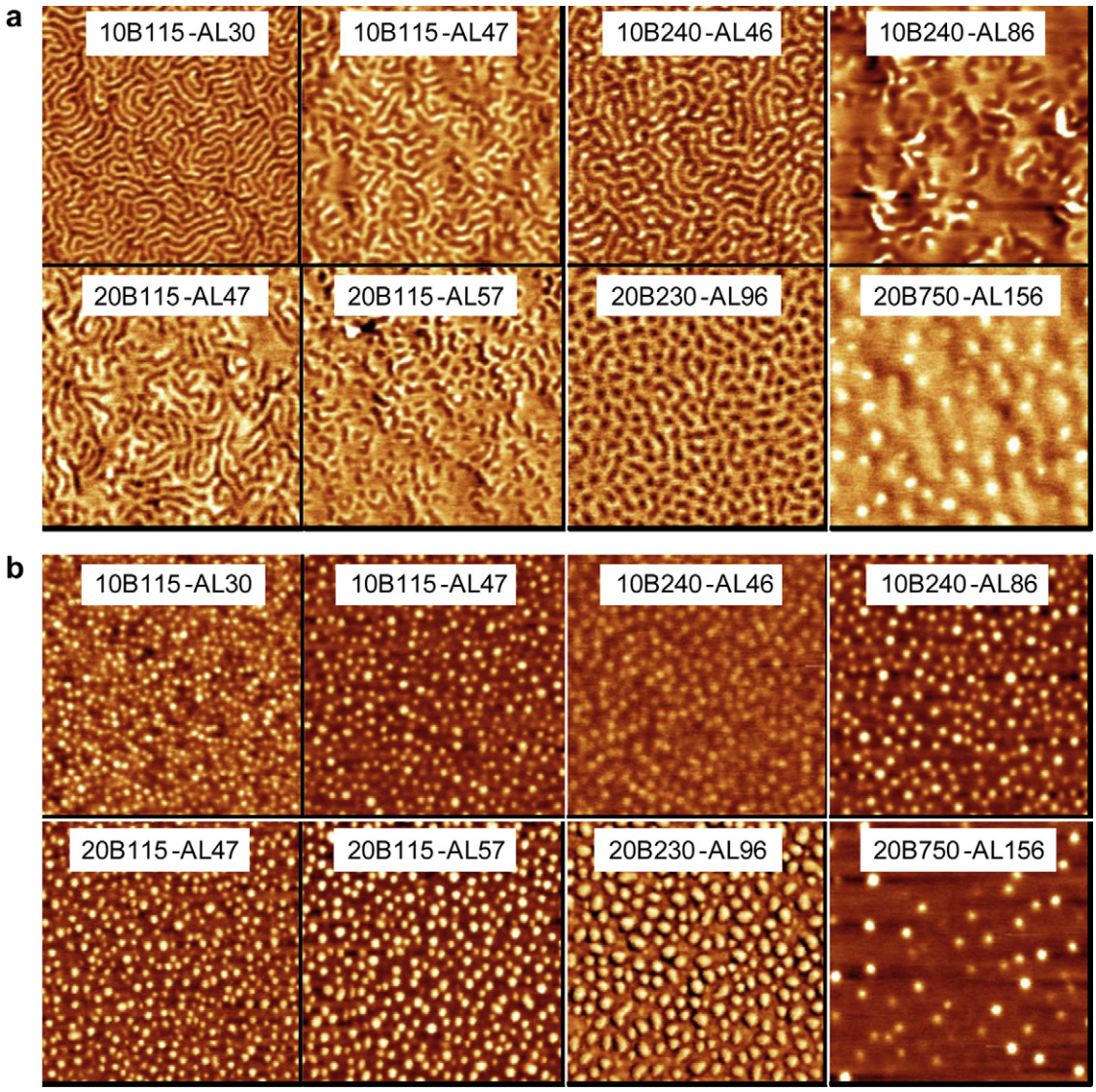

Fig. 4. Phase mode AFM images of film samples. (a) Images taken before annealing. (b) Images taken after annealing. Annealing conditions: 230 °C, 30 min, under N_2 flow, slow cooling down to room T. Image size = 1.0 × 1.0 μm^2. Brighter areas correspond to PMBL phase.

temperature dependencies of the real (G′) and the imaginary (G″) parts of the complex shear modulus at constant deformation frequency of 10 rad/s and heating rate of 2 °C/min.

Typical results for copolymers of constant PBA content and different PMBL block lengths are shown in Fig. 6. Two distinct glass transition temperatures corresponding to that of PBA ($T_g \sim -50$ °C) and PMBL ($T_g \sim 195$ °C) segments were observed in the DMA spectra for most copolymers that is a further evidence for their microphase-separated morphology. However, the glass transition of PMBL becomes less obvious with decreasing its content in the copolymers and, as can be seen in the Fig. 6, is barely detectable for 10B240-AL46.

With respect to the mechanical properties, all samples were glassy below the glass transition temperature of PBA, with storage modulus G′ ∼ 1 GPa. Above this glass transition, the copolymers become elastic and show a G′ plateau extending up to the glass transition temperature of PMBL (∼195 °C). In this elastic state the PMBL blocks form glassy domains connecting the flexible PBA matrix and serving as physical cross-links in a way typical for a thermoplastic elastomer. Finally, both storage and loss moduli decrease above the T_g of PMBL but the copolymers did not flow in the entire temperature range of up to 330 °C. The classical SBS and SIS thermoplastic elastomer systems exhibit phase separation that may also persists beyond the upper (PS) glass transition temperature [3]. However, above a certain temperature (ODT), the phase separation disappears and a monophase fluid is formed. This process known as ODT and is observed for most block copolymers [38–41]. For example, in their extensive work on the methacrylate–alkylene–methacrylate triblock copolymer thermoplastic elastomers [12,42–44] Jerome et al. showed that depending on the degree of miscibility of PMMA with poly (alkyl acrylate)s the ODT temperature in these systems may exceed 200 °C. In this respect the results shown in Fig. 6 demonstrate that the star-like PBA-*b*-PMBL copolymers maintain their microdomain morphology and elastic properties up to a very high ODT temperature of more than 330 °C, i.e., ∼130 °C above the glass transition of the PMBL. Thus the very high glass transition temperature and high thermal stability [26] of PMBL make the PMBL based thermoplastic elastomers particularly suitable for high temperature applications.

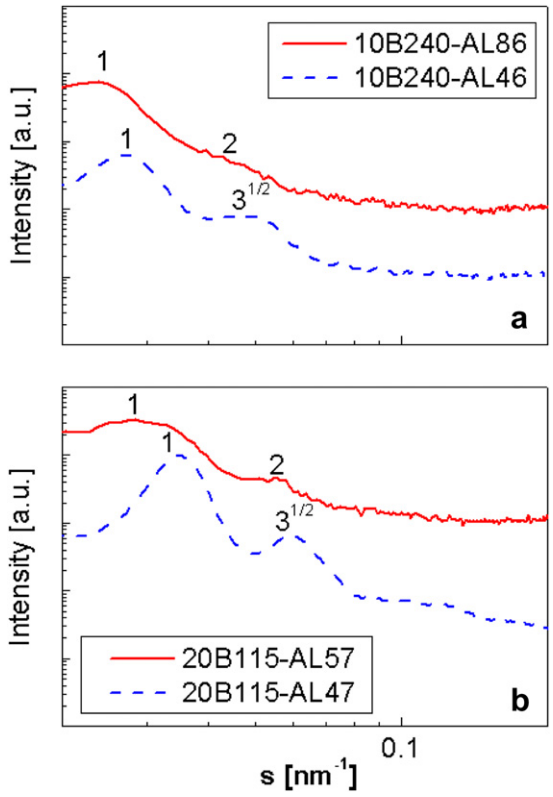

Fig. 5. SAXS spectra 10 and 20 arm star-like PBA–PMBL block copolymers measured after annealing at 150 °C.

The elasticity of the copolymers, i.e. the height of the rubbery plateau, strongly depends on the PMBL content. As seen in Fig. 6 the value of G′ at the rubber plateau region is approximately 0.1 MPa for the copolymers with PMBL fraction of 12.7 wt% (10B240-AL46) and up to approximately 10 MPa for the copolymers with PMBL content of 21.6 wt% (10B240-AL86).

The same effect is observed when studying the tensile properties of these materials. The measured stress–strain dependencies plotted in Fig. 7 show that both the initial modulus (E) and the tensile strength (σ break) increase with PMBL content that suggest a simple way of tuning these properties by adjusting copolymer composition. The ultimate tensile strength and elongation at break of the PBA–PMBL star block copolymers are significantly lower than those of the classical SIS and SBS thermoplastic elastomers with comparable molecular weights. While problems with the

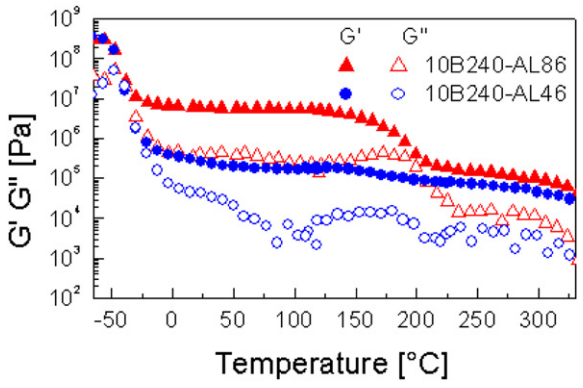

Fig. 6. Temperature dependence of shear moduli of PBA–PMBL star-like block copolymers with different compositions.

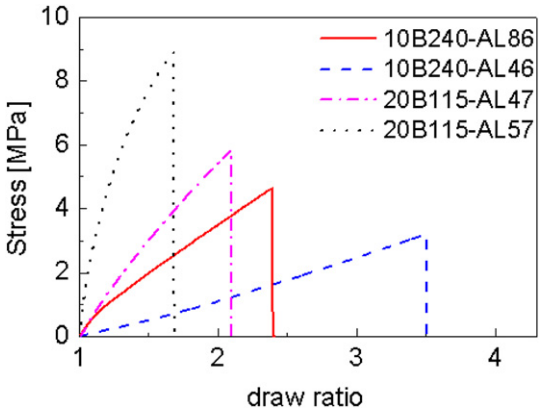

Fig. 7. Tensile mechanical properties of star-like block copolymers with different number of arms and compositions.

synthesis of the PBA–PMBL stars such as incomplete functionalization or relatively high polydispersity may decrease their tensile properties there is also more important fundamental reason for this difference. As discussed before [12,42–44], the molecular weigh between chain entanglements, M_e, of the soft PBA block is much higher than those of the central polybutadiene/polyisoprene blocks in the SBS/SIS. Since the number of chain entanglements is limited in the PBA–PMBL systems, the deformation stress is not dissipated by the soft PBA block, but directly transferred to the hard PMBL microdomains. Furthermore, the intrinsic brittleness of the hard PMBL blocks [26] may also have a negative effect on the ultimate tensile strength and elongation at break.

It was previously reported that thermoplastic elastomers based on star block copolymers may exhibit superior properties in comparison with the linear ABA triblock type TPEs [8,29–33]. In an attempt to explore these effects for PBA–PMBL based materials, we compared the newly synthesized 10 arm 10B115-AL30, 10B115-AL47 and 10B240-AL46 copolymers with linear PMBL-*b*-PBA-*b*-PMBL block copolymers with similar composition and arm molecular weight and prepared previously also using ATRP [15]. As shown in Table 3, there is more than double increase in both ultimate tensile strength and the elongation at break with the increase of number of arms from 2 up to 10.

Further increasing number of arms from 10 up to 20 has showed little influence on the mechanical properties. These results are not very surprising in view of earlier studies of polystyrene-*b*-polyisobutylene [31] and polystyrene-*b*-polydiene [45] star-like copolymers that have shown a saturation point in the improvement of the mechanical properties with respect to number of arms at $N_{arm} \sim 5–10$. In our case, both 10 and 20 arm star-like polymers fall in the region where the effect of N_{arm} is minor. This finding is also consistent with our recent studies of star-like PBA-*b*-PMMA copolymers, for which only minor effect of the number of arms on the mechanical properties was observed for $N_{arm} = 10$ and 20 [34].

Table 3
Ultimate Tensile Strength and Elongation at Break of linear and star-like PBA-*b*-PMBL Block Copolymers of Similar Composition.

Sample	Composition	PMBL content (wt%)	Ultimate tensile strength σ (MPa)	Maximum elongation at break λ (%)
BA215-AL68[15]	2 arms $PBA_{107.5}$-*b*-$PMBL_{34}$	19.3	1.9	55
10B115-AL30	10 arms PBA_{115}–*b*-$PMBL_{30}$	16.5	3.1	140
10B115-AL47	10 arms PBA_{115}–*b*-$PMBL_{47}$	24.2	7.8	140
BA375-AL60[15]	2 arms $PBA_{187.5}$-*b*-$PMBL_{30}$	10.9	0.7	100
10B240-AL46	10 arms PBA_{240}–*b*-$PMBL_{46}$	12.7	3.3	250

4. Conclusions

In summary, star-like 10 and 20 arm PBA macroinitiators were extended with outer hard PMBL block in order to prepare star-like thermoplastic elastomers. Halogen exchange strategy was applied during the ATRP of PMBL to provide at least equal rate of cross-propagation compared to rate of propagation. Partial star coupling during PBA arms extension with PMBL blocks was observed, and the coupling increased with number of arms and arm length. The morphology of solution cast films of the star-like PBA–PMBL block copolymers was studied by AFM and SAXS. Both techniques revealed a phase separated morphology of either cylindrical PMBL domains hexagonally arranged in the PBA matrix or lamellar morphology in the samples with higher content of PMBL (21–27 wt %). After annealing at 230 °C (over T_g of PMBL) the change of morphology leading to PMBL cylinders oriented perpendicularly to the surface was observed for all star-like copolymers. The mechanical and thermal properties of the star-like block copolymers have been thoroughly characterized. These materials possess typical elastomeric behavior in a broad range of service temperatures maintaining phase separated morphology even over 300 °C. Both the ultimate tensile strength and elongation at break of the 10 and 20 arm star-like PBA–PMBL copolymers are significantly higher than those of their linear ABA type counterparts with similar composition, indicating a strong effect of the higher number of arms on the mechanical properties. Even though the elongation at break is still lower than for commercial SBS or SIS thermoplastic elastomers, thanks to the very high glass transition temperature, high thermal stability of PMBL and higher polarity of methacrylates, these materials could be suitable for some special high temperature applications.

Acknowledgements

The financial support from National Science Foundation (DMR 09-69301 and CBET 06-09087) is greatly appreciated.

References

[1] Fetters LJ, Morton M. Macromolecules 1969;2:453–8.
[2] Holden G, Bishop ET, Legge NR. J Polym Sci Polym Symp 1969;26:37–57.
[3] Holden G, Legge NR. In: Holden G, Legge NR, Quirk RP, Schroeder HE, editors. Thermoplastic elastomers. 2nd ed. Munich, Germany: Hanser; 1996. p. 71.
[4] Jerome R, Fayt R, Teyssie P. In: Legge NR, Holden G, Schroeder HE, editors. Thermoplastic elastomers. Munich, Germany: Hanser; 1987.
[5] Malhotra SL, Lessard P, Blanchard LP. J Macromol Sci Chem 1981;A15:121–41.
[6] Cunningham RE. J App Polym Sci 1978;22:2907–13.
[7] Kobayashi S, Kataoka H, Ishizone T, Kato T, Ono T, Kobukata S, et al. Macromolecules 2008;41:5502–8.
[8] Shim JS, Kennedy JP. J Polym Sci Part A Polym Chem 2000;38:279–90.
[9] Jerome R, Bayard P, Fayt R, Jacobs C, Varshney S, Teyssie P. In: Holden G, Legge NR, Quirk RP, Schroeder HE, editors. Thermoplastic elastomers. Munich, Germany: Hanser; 1996.
[10] Moineau C, Minet M, Teyssie P, Jerome R. Macromolecules 1999;32:8277–82.
[11] Matyjaszewski K, Shipp DA, McMurtry GP, Gaynor SG, Pakula T. J Polym Sci Part A Polym Chem 2000;38:2023–31.
[12] Tong JD, Leclere P, Doneux C, Bredas JL, Lazzaroni R, Jerome R. Polymer 2000;41:4617–24.
[13] Matyjaszewski K, Spanswick J. Thermoplastic elastomers by controlled/living radical polymerization. In: Holden G, Kricheldorf HR, Quirk RP, editors. Thermoplastic elastomers. Munich, Germany: Hanser; 2004. p. 365.
[14] Braunecker WA, Matyjaszewski K. Prog Polym Sci 2007;32:93–146.
[15] Mosnáček J, Yoon JA, Juhari A, Koynov K, Matyjaszewski K. Polymer 2009;50:2087–94.
[16] Wang JS, Matyjaszewski K. J Amer Chem Soc 1995;117:5614–5.
[17] Kamigaito M, Ando T, Sawamoto M. Chem Rev 2001;101:3689–746.
[18] Matyjaszewski K, Xia JH. Chem Rev 2001;101:2921–90.
[19] Tsarevsky NV, Matyjaszewski K. Chem Rev 2007;107:2270–99.
[20] Matyjaszewski K, Tsarevsky NV. Nat Chem 2009;1:276–88.
[21] Mosnáček J, Matyjaszewski K. Macromolecules 2008;41:5509–11.
[22] van Rossum MWPC, Alberda M, van der Plas LHW. Phytochemistry 1998;49:723–9.
[23] Wong HF, Brown GD. Phytochemistry 2002;59:99–104.
[24] Trendafilova A, Todorova M, Mikhova B, Vitkova A, Duddeck H. Phytochemistry 2006;67:764–70.
[25] Akkapeddi MK. Macromolecules 1979;12:546–51.
[26] Brandenburg CJ. US6841627; 2005.
[27] Pickett JE and Ye Q. US2007/122625; 2007.
[28] Schwind H, Hauch D, Hasskerl T, Dorn K, and Hopp M. US5880235; 1999.
[29] Shim JS, Asthana S, Omura N, Kennedy JP. J Polym Sci Part A Polym Chem 1998;36:2997–3012.
[30] Storey RF, Shoemake KA. J Polym Sci Part A Polym Chem 1998;36:471–83.
[31] Shim JS, Kennedy JP. J Polym Sci Part A Polym Chem 1999;37:815–24.
[32] Dufour B, Koynov K, Pakula T, Matyjaszewski K. Macromol Chem Phys 2008;209:1686–93.
[33] Dufour B, Tang CB, Koynov K, Zhang Y, Pakula T, Matyjaszewski K. Macromolecules 2008;41:2451–8.
[34] Nese A, Mosnáček J, Juhari A, Yoon JA, Koynov K, Kowalewski T, et al. Macromolecules 2010;43:1227–35.
[35] Keller RN, Wycoff HD. Inorg Syn 1946;2:1–4.
[36] Tang W, Kwak Y, Braunecker W, Tsarevsky NV, Coote ML, Matyjaszewski K. J Amer Chem Soc 2008;130:10702–13.
[37] Matyjaszewski K, Shipp DA, Wang JL, Grimaud T, Patten TE. Macromolecules 1998;31:6836–40.
[38] Helfand E, Wasserman ZR. Macromolecules 1976;9:879–88.
[39] Leibler L. Macromolecules 1980;13:1602–17.
[40] Floudas G, Pakula T, Fischer EW, Hadjichristidis N, Pispas S. Acta Polym 1994;45:176–81.
[41] Floudas G, Pakula T, Velis G, Sioula S, Hadjichristidis N. J Chem Phys 1998;108:6498–501.
[42] Tong JD, Jerome R. Polymer 2000;41:2499–510.
[43] Tong JD, Leclere P, Rasmont A, Bredas JL, Lazzaroni R, Jerome R. Macromol Chem Physic 2000;201:1250–8.
[44] Tong JD, Leclere P, Doneux C, Bredas JL, Lazzaroni R, Jerome R. Polymer 2001;42:3503–14.
[45] Bi LK, Fetters LJ. Macromolecules 1976;9:732–42.